Geophys. J. Int. (1990) **100**, 423–431

Plate dynamics: Caribbean map corrections and hotspot push

J. F. Harper

Mathematics Department and Research School of Earth Sciences, Victoria University of Wellington, PO Box 600, Wellington, New Zealand

Accepted 1989 September 18. Received 1989 August 2; in original form 1988 December 19

SUMMARY

In 1986 the author's previous paper describing a simple mathematical model for the forces driving the plates had an rms error of 1.62 per cent in its best case. The model included slab pull and its global and local reactions proportional to speed times $(\text{age})^{3/2}$, viscous drag due to shear under moving plates and in the flow towards mantle sinks at midocean ridges and sources at subduction zones, ridge push proportional to plate age, and friction at continental collision zones. Strengths of the various forces were found by least-squares fitting. Three different improvements now reduce the error to 1.14 per cent. They are (1) revision of the N–S American plate boundary east of the Caribbean sea to run along the 15° 20′ fracture zone, (ii) removal of a transform segment from the Caribbean subduction zone, and (iii) allowing for 'hotspot push'. Hotspots cause upward flow in the mantle, which spreads outwards under the lithosphere above, and pushes two plates apart if their boundary runs nearby, in a way which is calculated.

The results and their statistical significance are estimated by a method given by Backus, Park & Garbasz (1981), modified slightly because three of the equations in the model are linearly dependent on the remainder. All the physical mechanisms envisaged in this work as driving plates turn out to be significant except local reaction to slab pull, the effect of which is very small anyway.

Key words: Caribbean, hotspots, North America, plate dynamics, South America.

1 INTRODUCTION

One way to investigate what drives the plates is to take a simplified mathematical model of the forces acting, calculate the velocities it predicts, and compare them with observation. Harper (1975a) and Gordon, Cox & Harter (1978) both did this and found errors of 20–30 per cent. Part of the reason for such large errors is that a small absolute error in any of the forces on a slow-moving plate causes a large change in its velocity. A better way to assess the forces acting was pioneered by Forsyth & Uyeda (1975): to take the velocities as given, use them to help estimate both driving and resisting torques about the centre of the Earth, and calculate the misfit between them for each plate in turn. In this way Forsyth & Uyeda (1975) achieved an rms misfit of 4.2 per cent, and subsequent workers have obtained even better results: 4.1 per cent (Chapple & Tullis 1977), 2.8 per cent (Harper 1978) and 1.62 per cent (Harper 1986).

The last paper actually reported 1.54 per cent, but all its misfit estimates should be multiplied by 1.05 for the following reason. The misfits were defined as percentages of the largest driving torque component, which at the present day is the Pacific z component (about the polar axis). That component had been calculated from Harper's (1986) tables 2 and 3 and their analogues for models not reported in such detail, but those tables do not give slab pull $\mathbf{M}_{\sigma j}$, local reaction $\mathbf{M}_{vj}$ and global reaction $\mathbf{M}_{\omega j}$ separately, only the combinations $(\mathbf{M}_{\sigma j}+\mathbf{M}_{vj})$ and $(\mathbf{M}_{\omega j}-\mathbf{M}_{vj})$. For the Pacific z component, $\mathbf{M}_{\sigma j}$ and $\mathbf{M}_{vj}$ were driving and $\mathbf{M}_{\omega j}$ resisting, and allowing for this gave the factor of 1.05 referred to. Even with this correction, the misfits were a considerable improvement on the previous work.

One of the conclusions of Harper (1986) was that the coefficients of $(\mathbf{M}_{\sigma j}+\mathbf{M}_{vj})$ and $(\mathbf{M}_{\omega j}-\mathbf{M}_{vj})$ were nearly equal. Hence $\mathbf{M}_{vj}$ contributes much less to the torque balance than $\mathbf{M}_{\omega j}$, and it would be more physically revealing to group slab pull and its reactions in the combinations $(\mathbf{M}_{\sigma j}+\mathbf{M}_{\omega j})$ and $(\mathbf{M}_{vj}-\mathbf{M}_{\omega j})$, in the expectation that the latter would be small by comparison with the former. That grouping of terms is adopted in this paper.

Harper's (1986) model incorporated the following physical effects: slab pull and global and local reactions duly weighted for $(\text{age})^{3/2}$ and speed, shear flow drag, source and sink drag, ridge push (using the age of the older plate at each boundary, with continent treated as 250 Ma ocean) and continental collision-zone friction. Full details are given by

Harper (1986, 1989), but some matters are worth mentioning here. The theory depends on approximations which are valid if the mesosphere is about 10–100 times as viscous as the asthenosphere, which seems likely from the work of Sabadini & Boschi (1981), Sabadini, Yuen & Boschi (1982, 1984), Hager (1984), Peltier (1986) and Bills & May (1987). This moderate viscosity contrast is the main reason for the differences between Harper's 1978 and 1986 papers. The former neglected any flow beneath the asthenosphere, which is realistic only for a viscosity ratio over 1000 (Davies 1977; Jacoby 1978), and which leads to source and sink drag and local slab reaction being found with the aid of the irrotational sources, sinks and vortices of Jacoby (1973) and Harper (1975b, 1978). In the more recent work (Harper 1986), flow can go down into the mesosphere and decreases more rapidly with distance from its lithospheric causes, and so the forces on the plates are more localized. For the same reason, flow induced by the weight of dipping slabs can go under them as well as horizontally around their ends, with the same consequence. However the viscosity contrast is still large enough for shear flow due to plate motion to be predominantly in the asthenosphere, and calculated the same way as in the earlier work. A transcription error was found in Harper (1986): his equation (22) for the torque due to source and sink flow should read

$$\mathbf{M}_s = -sR \int \frac{\mathbf{r} \times \mathbf{v}}{|\mathbf{v}|} |\boldsymbol{\omega}_{\mathrm{rel}} \cdot d\mathbf{l}|. \qquad (1)$$

The $\mathbf{r}\times$ in equation (1) above was missing. Fortunately, his computations used the correct form. His dimensionless $\mathbf{M}^*_{sj}$ is then

$$\mathbf{M}_s / sR^3\omega_0 \qquad (2)$$

where $\omega_0 = 1° \mathrm{Ma}^{-1}$, if the integral in equation (1) is taken around the boundary ∂P_j of plate number j.

We now turn to the differences between the present model and the earlier one; Section 2 describes those which concern the plate map, Section 3 the effect of a hotspot on the plate motion above it, Section 4 the methods for calculating the model's parameters and assessing their significance, and Section 5 gives the results of the calculations with various combinations of the parameters.

2 PLATE CARTOGRAPHY

2.1 The Caribbean subduction zone

Harper (1975a, 1978, 1986) used the intermediate-depth seismicity (Barazangi & Dorman 1969; ESSA/CGS 1970) to locate subduction zones. This puts the ends of the Caribbean zone near the points A and G on Fig. 1, but the segment EG is very close to a pure strike–slip boundary, and one might well suspect that the subducting plate goes down only along the segment ACE. The question is investigated dynamically below, by calculating torque balances on each of the hypotheses AG and AE.

2.2 The North–South American boundary

Locating the boundary between the North and South American plates has caused trouble ever since it was suggested that they were not one large plate. There are several fracture zones joining the mid-Atlantic ridge to the Caribbean subduction zone, and any of them might be the boundary in question. Ball & Harrison (1970) placed the boundary near 20°N, as did Harper (1978, 1986) along the dotted line GH (Fig. 1) which does have more seismicity than the obvious alternatives. At the other extreme, Collette *et al.* (1984) chose 10°N or even further south, while Vogt & Perry (1981) suggested 13°45°N, Le Douaran & Francheteau (1981) 13°N, Bowin (1976) 16°N at the Caribbean end, Stein & Gordon (1984) somewhere near 15°N and Roest & Collette (1986) the 15°20′ fracture zone. The geological arguments for this last alternative seem more cogent than the others, but the point is worth investigating dynamically also.

This paper takes four possibilities: AB, CD, EF, GH in Fig. 1, which meet the Caribbean arc at 11°, 14°, 17° and

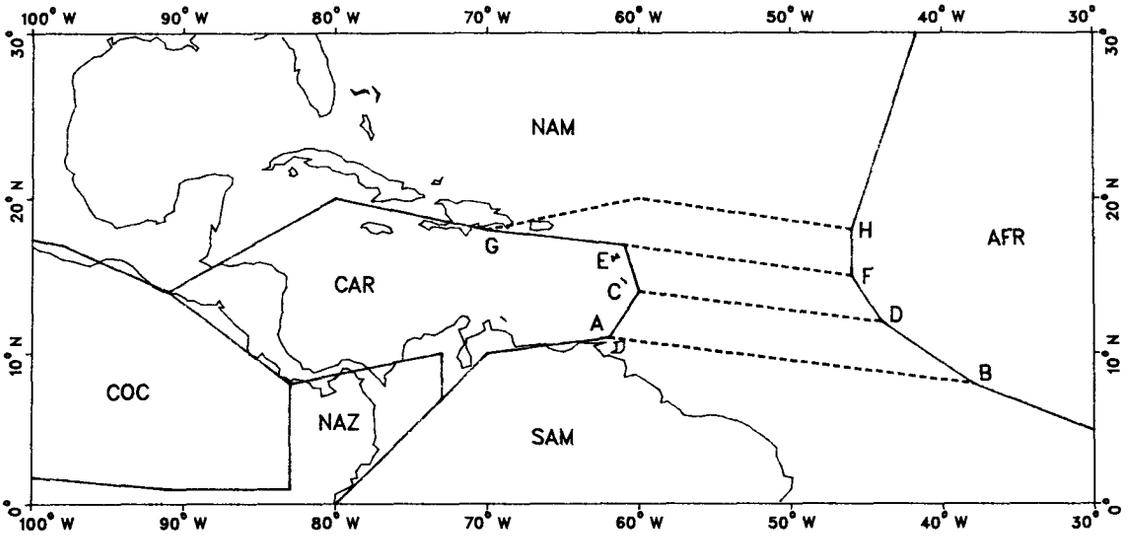

Figure 1. The Caribbean region. Dashed lines show alternative possible N–S American boundaries.

18°N and the mid-Atlantic ridge at 8°, 12°, 15° and 18° respectively; they all follow the trend of fracture zones in this region, and all coordinates were rounded to the nearest degree.

3 HOTSPOTS

While Harper's (1986) misfits between driving and resisting torques look quite small by the standards of previous work in the field, they were still large enough and concentrated enough around the Atlantic to suggest some systematic error. One obvious candidate is the mantle flow due to inhomogeneities other than those in the plates themselves. Two ways to investigate the inhomogeneities present themselves; tomography and hotspots. Tomography (see Dziewonski & Anderson 1984; Anderson & Dziewonski 1984, and a recent review by Lay 1987) has great promise but has not yet given results conclusive in the present context, and there seems to be no way to use it all for past geological reconstructions. Hotspots, on the other hand, can be traced back through the Cenozoic and most of the Mesozoic. If Morgan (1972) is correct, they cause rising plumes in the mantle, which spread outwards in all directions at the top. Such a flow in a viscous medium must help to push apart two plates whose boundary is nearby. The idea has been disputed (Runcorn 1974), but Olson & Singer (1985) have disposed of two of Runcorn's chief objections. Motion in the mantle due to other causes need not upset the regular progression in which individual blobs of rising hotspot material reach the top, and the blobs do not break up as they rise.

Hotspots have been defined in the past in two different ways. Morgan (1971, 1972) called them 'surface manifestations of lower mantle convection', but later he shifted his viewpoint downwards and defined them as 'those places in the mantle that produce midplate volcanism' (Morgan 1981). This paper adopts the second definition, in which a hotspot is a place in the mantle which is hotter, and so less dense, than its surroundings; one of the matters to investigate is how deep those places are. Each hotspot is presumably connected to its 'surface manifestation' by a mantle plume, and another matter to investigate is whether the density anomaly is primarily in the hotspot at the bottom or whether it is distributed up the plume. The tomographic work mentioned in the previous paragraph suggests that the most important density anomalies in the mantle, apart from those associated directly with plate boundary processes, are near depths of either 670 or 2800 km.

To model the flow due to a hotspot, we assume the hotspot to be a small region of the mantle less dense than its surroundings, and use the calculations of Harper (1986) Section 2 for the flow due to a vertical point force of unit strength (the Archimedes upthrust). If r is distance from the centre of the Earth scaled so that the Earth's radius is $r = 1$, we take the viscosity to be η_a = constant in the asthenosphere; $0.9 = a < r < 1$, but $100\eta_a$ in the mesosphere; $0.545 = c < r < a$. As in Harper (1986) the core's viscosity is assumed to be negligibly small, and the boundary at $r = a$ is assumed not to be an obstacle to flow except for the higher viscosity beneath it, so that the velocity and stress are continuous across $r = a$, and the normal velocity component is not assumed to be zero. (If it were, because the mantle had a chemical discontinuity at 670 km or so, one would be driven back to a theory like that of Harper 1978 which agrees less well with observation.)

The natural method for solving this problem in fluid mechanics is with a series in powers of r times appropriate Legendre functions of $\cos\theta$, where θ is the angular distance between a point in the mantle 'fluid' and the hotspot. In the present problem, it converges too slowly to be useful, especially as hotspots are giving only a small correction to the forces previously thought to be acting on the plates. Instead, one uses the series to find simpler empirical approximations to the potential φ of shear stress acting on the lithosphere in terms of the hotspot's distance b from the centre of the Earth (in the same units as above, so that $c < b < 1$) and a, c, θ as defined above. The following were used in what follows: for $a < b < 1$ (hotspot in the asthenosphere)

$$\varphi = -\frac{(1-b)^2}{8\pi b(1-2b\cos\theta + b^2)^{3/2}}, \tag{3}$$

and for $c < b < a$ (hotspot in the mesosphere)

$$\varphi = \beta\{1 - \exp[(1-\cos\theta)\alpha/\beta]\}, \tag{4}$$

where $\alpha = 210$, 16.5 and 0.155, $\beta = 0.9887$, 0.2822 and 9.052×10^{-3} for hotspots of unit strength at 670, 1200 and 2800 km depth, respectively. Equation (3) would be exact if the entire interior of the Earth had the same viscosity; it is within 10 per cent of the true value for all θ for the hotspot at 400 km. Equation (4) is merely a convenient simple approximation whose error is everywhere less than 6 per cent of β. Fig. 2 shows the variation of both the accurate and the approximate values of φ between 0° and 30°: beyond this φ merely increases monotonically towards its limiting value.

Because φ varies rapidly with θ near $\theta = 0$, the coarse digitization used for the world map was inadequate for finding $\int \varphi\, d\mathbf{r}$ around a plate boundary, which is proportional to the torque on the plate. Instead, each plate boundary segment was divided into four equal parts and the value of φ found at the mid-point of each. Two parts gave misleading results, especially for shallow hotspots; eight

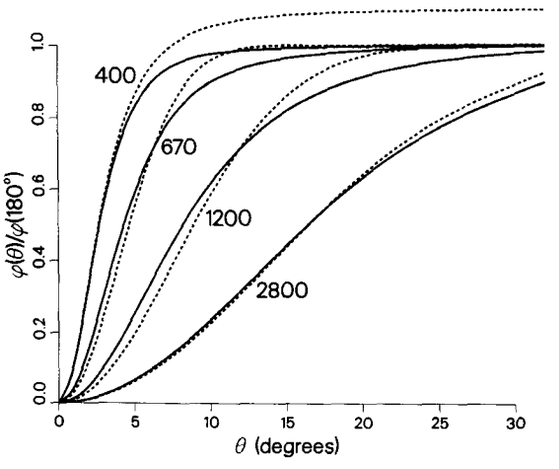

Figure 2. Graph of $\varphi(\theta)/\varphi(180°)$ against θ for four different depths of hotspots. Solid curves: accurate solution. Dashed curves: approximate solution.

parts increased the computation time without significantly reducing the errors.

Integrals of a similar kind occur in the calculation of ridge push and continental collision-zone friction, but they do not cause such severe numerical problems. If one of the integrals is denoted by $\int T\,d\mathbf{r}$, Harper (1986) used for each plate boundary segment the vector between its ends multiplied by the mean of the values of T at the ends. This effectively associates a given T value with the whole vector between the boundary points on each side of it. The present work associates each T value with the vectors half-way along the great circles to the next (or from the previous) boundary point, thereby gaining in accuracy, and explaining some small discrepancies between what would otherwise be identical models here and in Harper (1986).

It remains only to locate the hotspots in latitude, longitude and depth. For latitude and longitude, Richards, Hager & Sleep (1988) gave a list of 47 hotspots which was used without change. For depth, Olson, Schubert & Anderson (1987) showed that hotspots should be near either 670 km or the bottom of the mantle. Calculations were done with 400, 670, 1200 and 2800 km to check this. 2800 km is about 100 km above the core–mantle boundary (CMB), but the effect on the lithosphere of a given vertical force tends to zero (Harper 1983) as that force approaches the CMB. The hotspots are shown in Fig. 3, except for Erebus which is too far south for this projection. Fig. 3 also shows the plate boundaries, which are the same as in Harper (1986) except in the Caribbean region. A few calculations were done with several point forces distributed along a vertical line, instead of just one for each hotspot, to simulate uniform line forces along the mantle plume.

4 SOLVING THE EQUATIONS

Let $\mathbf{N}_p$ be the number of plates, 13 according to Minster & Jordan (1978) or 14 according to Chase (1978) when supplemented by the Sandwich plate as by Harper (1978). Then the theory gives $N = 3N_p$ equations, one for each Cartesian component of torque on each plate, of the form

$$\sum_{k=1}^{K} A_{nk}F_k = 0, \qquad n = 1, \ldots, N, \tag{5}$$

in the notation of Backus *et al.* (1981), where K is the number of independent types of force acting, which is seven with and six without hotspots included. F_k are the components of the vector $\mathbf{F}$ of unknown strength factors, and A_{nk} of the $N \times K$ matrix $\mathbf{A}$ of coefficients determined by the plate geometry and dynamics as follows. For torque component number $i = 1, 2, 3$ on plate number $j = 1, 2, \ldots, N_p$, let $n = i + 3j - 3$, and then

$$\begin{aligned}
A_{n1} &= (\mathbf{M}^*_{\sigma j})_i + (\mathbf{M}^*_{\omega j})_i,\\
A_{n2} &= (\mathbf{M}^*_{vj})_i - (\mathbf{M}^*_{\omega j})_i,\\
A_{n3} &= (\mathbf{M}^*_{sj})_i,\\
A_{n4} &= (\mathbf{M}^*_{rj})_i,\\
A_{n5} &= (\mathbf{M}^*_{cj})_i,\\
A_{n6} &= (\mathbf{M}^*_{pj})_i,\\
A_{n7} &= (\mathbf{M}^*_{hj})_i,
\end{aligned} \tag{6}$$

where $(\cdot)_i$ denotes component i of the vector inside the parentheses. All the dimensionless $\mathbf{M}^*$ are as defined by

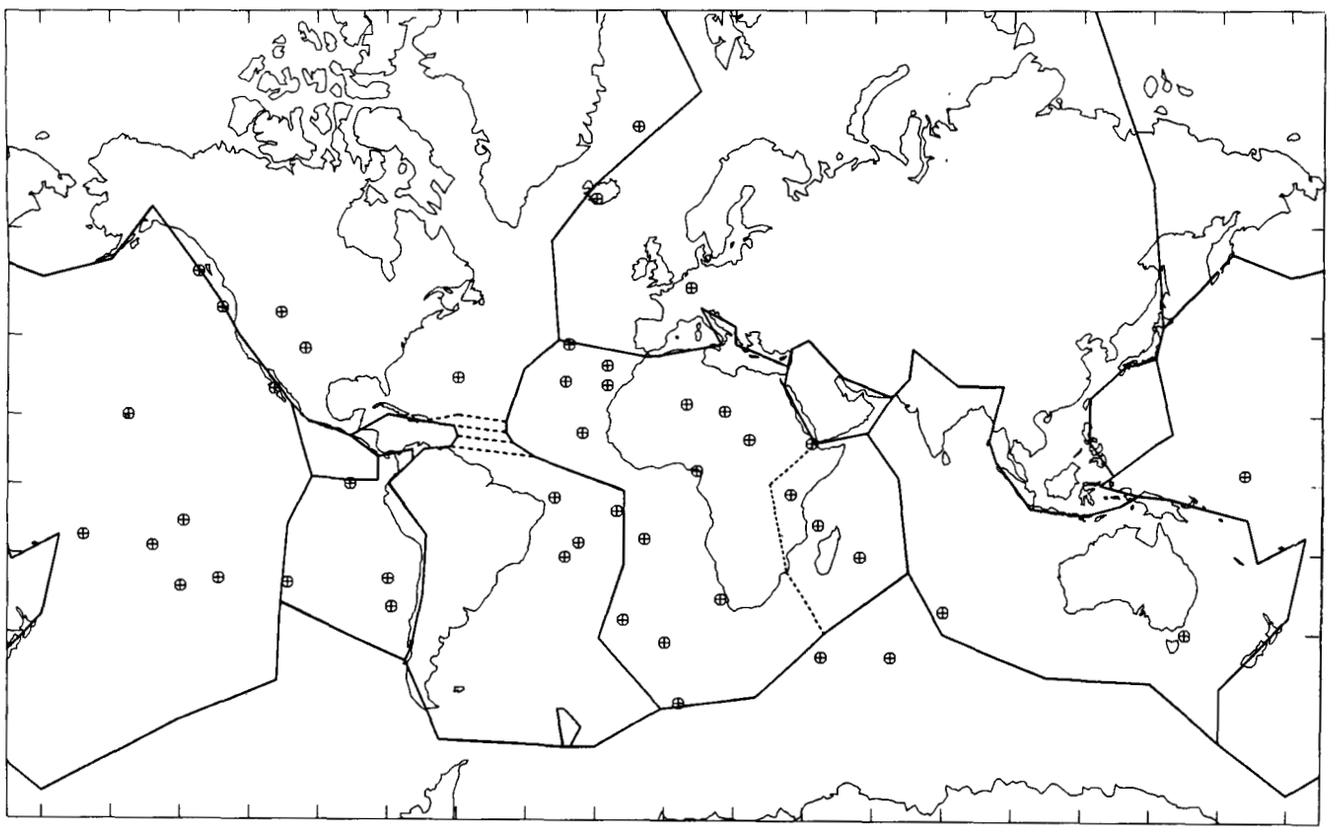

Figure 3. The world, showing plate boundaries and hotspots. Dashed lines show alternative possible boundaries.

Harper (1986) except $\mathbf{M}^*_{sj}$, the torque coefficient due to sources and sinks, which is given by equation (2), and $\mathbf{M}^*_{hj}$ which is given in terms of φ defined in equation (3) or (4) by

$$\mathbf{M}^*_{hj} = R^{-1}\int_{\partial P_j} \varphi d\mathbf{r}. \tag{7}$$

Harper (1986) used different definitions of A_{n1} and A_{n2}, namely $(\mathbf{M}^*_{oj})_i - (\mathbf{M}^*_{vj})_i$ and $-A_{n2}$ in the above notation. He found $\mathbf{F}$ by taking $F_1 = 1$ and minimizing the error norm $\mathbf{F}^T\mathbf{A}^T\mathbf{A}\mathbf{F}$. In this paper the method of Backus *et al.* (1981) will be used instead, so that their methods of assessing statistical significance can be applied, and to ensure that all the elements of $\mathbf{F}$ are treated alike.

Backus *et al.* (1981) began by normalizing the matrix $\mathbf{A}$ by dividing each column by its column norm W_k, where

$$W_k^2 = \sum_{n=1}^{N} A_{nk}^2,$$

to yield a second matrix $\mathbf{a}$ such that the $K \times K$ matrix

$$\mathbf{B} = \mathbf{a}^T\mathbf{a}$$

has its (lm) element equal to the correlation coefficient between the N-component vectors A_{nl} and A_{nm}.

If $f_k = N^{-1}W_kF_k$, equation (5) is equivalent to $\mathbf{af} = \mathbf{0}$, but as Backus *et al.* (1981) explained, there are errors in the estimation of parameters in $\mathbf{a}$ and possibly driving mechanisms for plates which should have been included but were not, and so $\mathbf{af}$ is not exactly zero for any non-zero $\mathbf{f}$. They showed that the optimal choice of $\mathbf{f}$ is then the eigenvector $\mathbf{v}_1$ of $\mathbf{B}$ with the smallest eigenvalue β_1. On the assumption of errors in the rows of $\mathbf{a}$ which all behave as if chosen independently from the same Gaussian distribution with mean zero, they estimated its variance as σ^2/N where

$$\sigma^2/N = \beta_1/(N - K + 1), \tag{8}$$

and they showed how to estimate the variance $(\delta v_{kl})^2$ of the kth component of the lth eigenvector v_{kl} as

$$(\sigma v_{kl})^2 = (\sigma^2/N)\sum_{j\neq l}(\beta_j^{(0)} + \beta_l^{(0)})(\beta_j^{(0)} - \beta_l^{(0)})^{-2}v_{kj}^2, \tag{9}$$

where $\beta_1^{(0)} = 0$, the least eigenvalue of the 'true' matrix $\mathbf{B}^0$ to which $\mathbf{B}$ is an approximation, and its other eigenvalues $\beta_j^{(0)}$ are estimated as the other eigenvalues β_j of $\mathbf{B}$, $j = 2, \ldots, K$. Backus *et al.* (1981) also showed how to check the probability of $\mathbf{B}^{(0)}$ really having the rank $K - 1$ assumed in deriving equations (8) and (9) and how to check for normality using the Kolmogorov–Smirnov test. Similar checks were done with all the models described in this paper and nothing untoward was found, as indeed nothing untoward was found when Backus *et al.* checked Forsyth & Uyeda's (1975) work; the problems with it lie elsewhere.

Backus *et al.* (1981) seem to have assumed when deriving

Table 1. Plate torque errors, smallest eigenvalues, and F_1 values (equation 4) for various models. C = Chase (1978), MJ = Minster and Jordan (1978), other pairs of letters refer to points on Fig. 1.

Plate model	NAM-SAM bdy.	Carib. subd. zone	Hotspot depth (km)	Cont'l equiv. age (Ma)	Max. error (%)	RMS error (%)	Least eigen-value	F_1
(a)								
MJ	GH	AG	-	250	5.41	1.61	.00484	.0000
MJ	GH	AE	-	250	5.31	1.56	.00459	.0011
MJ	EF	AE	-	250	5.03	1.50	.00431	.0024
MJ	CD	AE	-	250	5.10	1.53	.00445	.0037
MJ	AB	AE	-	250	5.03	1.55	.00461	.0057
MJ	AB	AG	-	250	5.13	1.57	.00472	.0048
(b)								
C	GH	AG	-	250	3.70	1.67	.00553	.0175
C	GH	AE	-	250	3.61	1.64	.00533	.0182
C	EF	AE	-	250	3.61	1.64	.00532	.0182
C	CD	AE	-	250	3.63	1.64	.00536	.0195
C	AB	AE	-	250	3.65	1.67	.00550	.0231
C	AB	AG	-	250	3.67	1.69	.00568	.0227
(c)								
MJ	EF	AE	400	250	4.07	1.38	.00377	-.0013
MJ	EF	AE	670	250	3.98	1.37	.00376	-.0003
MJ	EF	AE	1200	250	3.14	1.28	.00325	-.0023
MJ	EF	AE	2800	250	2.93	1.18	.00277	-.0039
(d)								
C	EF	AE	400	250	3.41	1.59	.00515	.0154
C	EF	AE	670	250	3.41	1.59	.00516	.0161
C	EF	AE	1200	250	3.35	1.54	.00488	.0132
C	EF	AE	2800	250	3.31	1.48	.00451	.0103
(e)								
MJ	EF	AE	2800	90	3.01	1.20	.00310	-.0662
MJ	EF	AE	2800	170	2.84	1.14	.00263	-.0194
MJ	EF	AE	2800	250	2.93	1.18	.00277	-.0039
MJ	EF	AE	2800	350	3.11	1.22	.00292	.0047
(f)								
C	EF	AE	2800	90	3.75	1.47	.00475	-.0493
C	EF	AE	2800	170	3.14	1.45	.00437	-.0045
C	EF	AE	2800	250	3.31	1.48	.00451	.0103
C	EF	AE	2800	350	3.39	1.51	.00466	.0186
(g)								
MJ	GH	AE	2800	170	2.97	1.12	.00254	-.0222
MJ	EF	AE	2800	170	2.84	1.14	.00263	-.0194
MJ	CD	AE	2800	170	2.84	1.16	.00270	-.0179
MJ	AB	AE	2800	170	2.78	1.17	.00280	-.0157

equations (8) and (9) and stating that $\beta_1 N/\sigma^2$ has a χ^2 distribution with $N-K+1$ degrees of freedom that all N equations (5) are linearly independent. In fact the world sum of torques on all the plates is zero, and so the sum of the $n/3$ coefficients A_{nk} is zero for each k if $n-i$ is divisible by 3, for $i=1, 2, 3$. It appears then that the number of degrees of freedom in the distribution of $\beta_1 N/\sigma^2$ and in equation (8) should be $(N-K-2)$, not $(N-K+1)$. This change has been made in what follows. The effect is to make the error estimates slightly worse than unmodified Backus *et al.* (1981) statistics would have done.

5 RESULTS

The main results of this study are given in Table 1. Its first column shows which plate model was used, either Minster & Jordan (1978) or Chase (1978). The next two columns indicate the N–S American boundary and the extent of the Caribbean subduction zone. Then come the depth of the hotspots and the oceanic equivalent age assumed for continental crust (Harper 1986). The last four columns summarize the computed results; the worst single error component and rms error as a percentage of the largest driving torque component, the smallest eigenvalue of the matrix **B**, and the value of the local reaction parameter F_1, where equations (5) and (6) show that the total torque on plate j due to slab pull and its local and global reaction is $\mathbf{M}_{\sigma j} + F_1\mathbf{M}_{vj} + (1-F_1)\mathbf{M}_{\omega j}$. Table 2 shows the eigenvalues and eigenvectors for matrix **B**.

Table 1(a) presents the results of models with no hotspots and 250 Ma equivalent continents, the best choice according to Harper (1986). It shows that EF on Fig. 1 is the best-fitting choice of plate boundary and AE rather than AG is the better location of the subduction zone (although it makes practically no difference if EF actually is the plate boundary because the section EG is then subducting so slowly that it has very little slab pull).

Table 1(b) gives the corresponding results for Chase's (1978) data instead of Minster & Jordan's (1978); the choice of plate geometry has much smaller effects here. Tables 1(c) and (d) explore the consequences of hotspots at the four different depths, while Tables 1(e) and (f) choose the optimal depth and explore different continental equivalent ages. Finally, Table 1(g) re-examines the plate geometry with the optimal hotspot depth and continental equivalent age, using Minster & Jordan's (1978) data. Details are not given in the table for vertical line distributions of hotspots; in every case they gave errors smaller than for a single hotspot at the top of the line, but a single hotspot at the bottom gave errors that were smaller still.

Table 3 gives detailed results from the best-fitting geologically likely case (plate boundary EF, subduction zone

Table 2. Matrix **B**, its eigenvalues and eigenvectors, eigenvector standard deviations, and ratios of first eigenvector components to standard deviations, for the model (MJ, EF, AE, 2800, 170) of Table 1.

Matrix **B**

1.0000	0.2201	-0.8369	-0.9832	-0.1409	0.5142	0.4718
0.2201	1.0000	-0.3983	-0.2320	-0.0407	0.3286	0.2583
-0.8369	-0.3983	1.0000	0.8583	0.1973	-0.7556	-0.5555
-0.9832	-0.2320	0.8583	1.0000	0.1307	-0.6121	-0.5431
-0.1409	-0.0407	0.1973	0.1307	1.0000	-0.4769	-0.0308
0.5142	0.3286	-0.7556	-0.6121	-0.4769	1.0000	0.4291
0.4718	0.2583	-0.5555	-0.5431	-0.0308	0.4291	1.0000

Eigenvalues

0.0026	0.1034	0.3491	0.6085	0.9188	1.1310	3.8865

Column eigenvectors

-0.6810	0.1245	-0.3261	-0.3065	-0.2892	-0.1848	-0.4501
0.0100	0.1019	-0.2329	-0.2473	0.9086	-0.0412	-0.2166
-0.1244	0.8250	-0.2337	0.1258	-0.0001	0.0472	0.4808
-0.6926	-0.3788	0.1388	0.1968	0.2592	0.1766	0.4695
-0.0695	0.0975	0.4690	-0.0882	0.0830	-0.8536	0.1496
-0.1832	0.3746	0.7107	0.0885	0.0868	0.3765	-0.4049
-0.0502	0.0109	-0.2011	0.8802	0.0962	-0.2456	-0.3356

Standard deviations

0.0083	0.0225	0.0169	0.0186	0.0190	0.0214	0.0048
0.0105	0.0128	0.0192	0.0349	0.0107	0.0578	0.0066
0.0245	0.0077	0.0219	0.0157	0.0124	0.0102	0.0044
0.0121	0.0211	0.0173	0.0157	0.0161	0.0189	0.0046
0.0110	0.0151	0.0132	0.0264	0.0547	0.0090	0.0071
0.0162	0.0195	0.0122	0.0277	0.0279	0.0130	0.0053
0.0114	0.0151	0.0314	0.0101	0.0366	0.0220	0.0058

Ratios

82.225	Slab pull + global reaction
0.950	Local - global reaction
5.086	Source & sink drag
57.336	Shear flow drag
6.292	Collision zone friction
11.307	Ridge push
4.404	Hotspot push

Table 3. Matrix of torque components, solution vector **F**, and misfit torques for the model (NJ, EF, AE, 2800, 170) of Table 1.

Plate	Slab pull +glob.	Local -glob.	Source & sink drag	Shear flow drag	Collision zones	Ridge push	Hotspots	Misfit
PAC	-0.1707	0.0011	0.0016	0.2581	-0.0115	-0.0651	0.0040	0.0176
	0.5511	-0.0025	-0.0789	-0.5815	-0.0118	0.1187	-0.0129	-0.0179
	-1.1865	0.0071	0.1801	1.1163	0.0108	-0.0828	-0.0489	-0.0039
AFR	0.0440	0.0005	-0.0014	-0.0849	-0.0011	0.0081	0.0192	-0.0154
	-0.2234	-0.0030	0.0027	0.2267	0.0555	-0.0935	0.0043	-0.0307
	0.2252	0.0039	-0.0170	-0.3076	-0.0006	0.0096	0.0408	-0.0456
EUA	-0.0527	0.0056	0.0511	0.0666	0.0558	-0.1376	-0.0305	-0.0418
	-0.1753	0.0004	0.0090	0.1996	-0.0928	0.0689	-0.0361	-0.0262
	0.1639	0.0031	-0.0113	-0.1863	0.0241	0.0082	0.0231	0.0248
IND	0.3304	0.0028	-0.0637	-0.3812	-0.0450	0.1537	0.0252	0.0222
	0.2168	0.0022	-0.0333	-0.2744	0.0290	0.0686	0.0059	0.0148
	0.3636	-0.0054	-0.0787	-0.3782	-0.0292	0.0994	0.0171	-0.0115
ANT	-0.0114	-0.0002	0.0423	0.0400	0.0	-0.0252	-0.0060	0.0395
	-0.1216	-0.0024	0.0449	0.0741	0.0	-0.0358	0.0288	-0.0119
	0.0398	0.0008	-0.0033	-0.0587	0.0	0.0129	0.0073	-0.0012
NAM	-0.0293	-0.0030	-0.0342	-0.0219	0.0281	0.0743	-0.0045	0.0095
	-0.0609	0.0050	0.0354	0.1767	-0.0171	-0.1123	-0.0047	0.0222
	0.0343	-0.0026	0.0017	0.0719	0.0161	-0.0889	-0.0081	0.0244
SAM	-0.0548	-0.0008	0.0121	0.0686	0.0094	-0.0328	-0.0059	-0.0043
	-0.0810	-0.0033	-0.0236	0.0590	0.0043	0.0515	0.0242	0.0312
	0.0865	0.0058	0.0672	0.0441	0.0038	-0.1364	-0.0471	0.0239
NAZ	-0.0258	-0.0001	-0.0104	0.0310	0.0092	0.0040	-0.0066	0.0012
	-0.0907	-0.0005	0.0370	0.0941	0.0022	-0.0353	-0.0016	0.0052
	0.2393	0.0012	-0.0927	-0.2428	-0.0010	0.0996	0.0052	0.0089
PHL	-0.0106	-0.0050	-0.0014	0.0041	0.0	0.0135	0.0001	0.0008
	-0.0068	0.0037	0.0054	0.0012	0.0	0.0009	0.0006	0.0050
	-0.0120	-0.0140	-0.0084	0.0114	0.0	0.0265	-0.0010	0.0024
ARB	0.0002	0.0000	-0.0068	-0.0151	-0.0263	0.0312	0.0033	-0.0134
	-0.0115	-0.0002	0.0078	0.0308	0.0372	-0.0442	-0.0093	0.0107
	0.0182	0.0004	-0.0039	-0.0292	-0.0212	0.0252	0.0101	-0.0005
CAR	-0.0034	-0.0003	-0.0076	0.0024	-0.0185	0.0241	0.0010	-0.0024
	0.0008	-0.0000	-0.0006	-0.0007	-0.0065	0.0057	0.0006	-0.0007
	0.0070	0.0001	0.0021	-0.0054	-0.0028	-0.0043	0.0009	-0.0024
COC	-0.0160	-0.0000	0.0252	0.0339	0.0	-0.0507	0.0007	-0.0069
	0.0031	0.0000	-0.0082	-0.0067	0.0	0.0097	-0.0001	-0.0023
	0.0204	0.0002	-0.0314	-0.0343	0.0	0.0288	0.0008	-0.0154
SAN	0.0001	-0.0006	-0.0069	-0.0015	0.0	0.0024	-0.0002	-0.0067
	-0.0005	0.0005	0.0023	0.0009	0.0	-0.0029	0.0003	0.0005
	0.0002	-0.0005	-0.0045	-0.0011	0.0	0.0023	-0.0002	-0.0038
F	1.0000	-0.0194	0.0577	0.7887	0.0272	0.0019	1.1035	

AE, hotspots at 2800 km), in a format similar to table 3 of Harper (1986). It is in the same units, i.e. the slab pull torque about the centre of the Earth per unit length of strike of lithosphere 100 Ma old subducting at $1°\,Ma^{-1}$ is assigned unit strength, and the normalizations described in Section 4 above have been undone. Their use was for finding the statistical significance of the results, not their physical magnitude.

6 DISCUSSION AND CONCLUSIONS

This study leads to the following conclusions.

(1) Minster & Jordan's (1978) kinematic data lead to smaller **B** eigenvalues and rms torque errors than Chase's (1978), and they are also more sensitive to changes in the other parameters. Their maximum error components are also smaller than Chase's in the better-fitting models, though not in the worse-fitting ones.

(2) All the physical mechanisms generating torques on the plates are statistically significant, being from 4.4 to 82 standard deviations away from zero in Table 2, except local slab reaction which is only 0.95 standard deviations from zero and whose physical effect is very small anyway (see Table 3). This is in sharp contrast with Forsyth & Uyeda (1975) as analysed by Backus *et al.* (1981). There only slab pull and friction at slab bottoms were significant, and all six of their other physical mechanisms were insignificant. The present work also has very much smaller errors: the variance ratio is $(36 \times 0.01080/29) \div (39 \times 0.002631/30) = 3.919$, which should follow an F-distribution with 29 and 30 degrees of

freedom. Even 3.25 would be significant at the 0.1 per cent level (Abramowitz & Stegun 1964); the probability is therefore greater than 0.999 that the present work is better than Forsyth & Uyeda (1975). A calculation of the integral defining the F-distribution gave the actual probability as 0.9995 correct to four figures.

(3) In every case the reaction parameter F_1 is close to zero. Positive values of F_1 suggest that the upper plate at a subduction zone is pulled towards the lower plate by a force per unit length of R times the slab pull; physically, this could be extra ridge push due to the abnormally deep ocean at trenches, causing Elsasser's (1971) retrograde motion or Forsyth & Uyeda's (1975) suction. Negative values of F_1 suggest that the lower plate pushes the upper plate away from the subduction zone, as would be expected for friction between the two plates in contact. Table 1(d) indicates a very small amount of net friction in the best-fitting models, but it is clearly not well constrained by the calculations given here. It is quite possible that suction and friction are both present, and the smallness of R implies that they nearly cancel out.

(4) The hotspots are at the bottom of the mantle according to the results in Table 1(c) and 1(d).

(5) The continents behave most nearly like oceanic crust of 170 Myr age.

(6) The Caribbean subduction zone fits the theory a little better if it extends from A to E rather than all the way from A to G; the difference in errors is small but consistent when other parameters are varied.

(7) The N–S American plate boundary along EF seemed initially to be suggested by the results (Table 1a), but by the time other parameters had been optimized (Table 1g) it appears that the position was not well constrained: GH gives a slightly smaller rms error but larger maximum error; AB is the other way around. The differences between the errors are insignificant. Geology (Roest & Collette 1986) is therefore a better way to locate this boundary.

(8) Hotspots reduce the errors and the smallest matrix eigenvalue considerably, but by an amount which is not quite statistically significant. With the Caribbean correction and with equivalent age of continental crust altered from 250 to 170 Ma as well, the total effect of this paper is to reduce the least eigenvalue from 0.00482 for the physical model of Harper (1986) treated by the present methods, as in the first line of Table 1, to 0.002631. At the same time the number of degrees of freedom has gone down from 31 to 30, giving a variance ratio of 1.781. The 10 per cent significance point for the relevant F-distribution is 1.62, the 5 per cent one is 1.84, and the actual ratio is between those values.

(9) By calculating their variance ratios and applying the F-test, it can be shown that in the sequence of papers Forsyth & Uyeda (1975), Harper (1978), Harper (1986) and this work, each is a statistically significant improvement not on the previous one but on the one before that. The significance levels are between 5 and 1 per cent from Forsyth & Uyeda (1975) to Harper (1986), and between 1 and 0.1 per cent from Harper (1978) to this paper.

(10) One feature has survived unchanged from Harper (1978, 1986) in spite of the changes in force models: the worst torque errors are on the large slow-moving continental plates. Africa, Eurasia and Antarctica come out worst in Table 3.

REFERENCES

Abramowitz, M. & Stegun, I. A., 1964. *Handbook of Mathematical Functions*, National Bureau of Standards Applied Mathematics Series 55, US Government Printing Office, Washington, DC.

Anderson, D. L. & Dziewonski, A. M., 1984. Seismic tomography, *Sci. Am.*, **251** (4), 58–66 and 146.

Backus, G., Park, J. & Garbasz, D., 1981. On the relative importance of the driving forces of plate motion, *Geophys. J.R. astr. Soc.*, **67**, 415–435.

Ball, M. M. & Harrison, C. G. A., 1970. Crustal plates in the central Atlantic, *Science*, **167**, 1128–1129.

Barazangi, M. & Dorman, J., 1969. World seismicity maps compiled from ESSA, Coast and Geodetic Survey, epicenter data, 1961–1967, *Bull. seism. Soc. Am.*, **59**, 369–380.

Bills, B. G. & May, G. M., 1987. Lake Bonneville: constraints on lithospheric thickness and upper mantle viscosity from isostatic warping of Bonneville, Provo and Gilbert stage sediments, *J. geophys. Res.*, **92**, 11 493–11 508.

Bowin, C., 1976. Caribbean gravity field and plate tectonics, *Spec. pap. geol. Soc. Am.*, **169**.

Chapple, W. M. & Tullis, T. E., 1977. Evaluation of the forces that drive the plates, *J. geophys. Res.*, **82**, 1967–1984.

Chase, C. G., 1978. Plate kinematics: the Americas, East Africa, and the rest of the world, *Earth planet. Sci. Lett.*, **37**, 355–368.

Collette, B. J., Slootweg, A. P., Verhoef, J. & Roest, W. R., 1984. Geophysical investigations of the floor of the Atlantic Ocean between 10° and 38°N (Kroonlag-project), *Proc. K. ned. Akad. Wet. Series B*, **87**, 1–76.

Davies, G. F., 1977. Whole-mantle convection and plate dynamics, *Geophys. J.R. astr. Soc.*, **49**, 459–486.

Dziewonski, A. M. & Anderson, D. L., 1984. Seismic tomography of the Earth's interior, *Am. Sci.*, **72**, 483–494.

Elsasser, W. M., 1971. Sea-floor spreading as thermal convection, *J. geophys. Res.*, **76**, 1101–1112.

ESSA/CGS, 1970. *Seismicity of the World*, US Department of Commerce, Environmental Science Services Administration, Coast and Geodetic Survey, *map sheets NEIC 3008–3021.*

Forsyth, D. W. & Uyeda, S., 1975. On the relative importance of the driving forces of plate motion, *Geophys. J.R. astr. Soc.*, **43**, 163–200.

Gordon, R. G., Cox, A. & Harter, E. C., 1978. Absolute motion of an individual plate estimated from its ridge and trench boundaries, *Nature*, **274**, 752–755.

Hager, B. H., 1984. Subducted slabs and the geoid: constraints on mantle rheology and flow, *J. geophys. Res.*, **89**, 6003–6015.

Harper, J. F., 1975a. On the driving forces of plate tectonics, *Geophys. J.R. astr. Soc.*, **40**, 465–474.

Harper, J. F., 1975b. Subduction-zone vortices, *Bull. Aust. Soc. Explor. Geophys.*, **6**, 79–80.

Harper, J. F., 1978. Asthenosphere flow and plate motions, *Geophys. J.R. astr. Soc.*, **55**, 87–110.

Harper, J. F., 1983. Axisymmetric Stokes flow images in spherical free surfaces with applications to rising bubbles, *J. Austral. Math. Soc. Ser. B*, **25**, 217–231.

Harper, J. F., 1986. Mantle flow and plate motions, *Geophys. J.R. astr. Soc.*, **87**, 155–171.

Harper, J. F., 1989. Forces driving plate tectonics: the use of simple dynamical models, *Rev. aquatic Sci.*, **1**, 319–336.

Jacoby, W. R., 1973. Model experiment of plate movements, *Nature Phys. Sci.*, **242**, 130–135.

Jacoby, W. R., 1978. One-dimensional modelling of mantle flow, *Pure appl. Geophys.*, **116**, 1231–1249.

Lay, T., 1987. Structure of the Earth: mantle and core, *Rev. Geophys.*, **25**, 1161–1167.

Le Douaran, S. & Francheteau, J., 1981. Axial depth anomalies from 10 to 50° north along the Mid-Atlantic Ridge: correlation

with other mantle properties, *Earth planet. Sci. Lett.*, **54,** 29–47.

Minster, J. B. & Jordan, T. H., 1978. Present-day plate motions, *J. geophys. Res.*, **83,** 5331–5354.

Morgan, W. J., 1971. Convection plumes in the lower mantle, *Nature,* **230,** 42–43.

Morgan, W. J., 1972. Deep mantle plumes and plate motions, *Bull. Am. Ass. Petrol. Geol.*, **56,** 203–213.

Morgan, W. J., 1981. Hotspot tracks and the opening of the Atlantic and Indian Oceans, in *The Oceanic Lithosphere,* pp. 443–487, ed. Emiliani, C., Wiley-Interscience, New York.

Olson, P. & Singer, H., 1985. Creeping plumes, *J. Fluid Mech.*, **158,** 511–531.

Olson, P., Schubert, G. & Anderson, D. L., 1987. Plume formation in the D"-layer and the roughness of the core–mantle boundary, *Nature,* **327,** 409–412.

Peltier, W. R., 1986. Deglaciation-induced vertical motion of the North American continent and transient lower mantle rheology, *J. geophys. Res.*, **91,** 9099–9123.

Richards, M. A., Hager, B. H. & Sleep, N. H. 1988. Dynamically supported geoid highs over hotspots: observation and theory, *J. geophys. Res.*, **93,** 7690–7708.

Roest, W. R. & Collette, B. J., 1986. The Fifteen Twenty Fracture Zone and the North American–South American plate boundary, *J. geol. Soc. Lond.*, **143,** 833–843.

Runcorn, S. K., 1974. On the forces not moving lithospheric plates, *Tectonophysics,* **21,** 197–202.

Sabadini, R. & Boschi, E., 1981. A geophysical discussion on the secular instability of the rotation pole, *Bull. Geofis. Teor. Appl.*, **23,** 238–296.

Sabadini, R., Yuen, D. A. & Boschi, E., 1982. Polar wandering and the forced responses of a rotating, multilayered, viscoelastic planet, *J. geophys. Res.*, **87,** 2885–2903.

Sabadini, R., Yuen, D. A. & Boschi, E., 1984. A comparison of the complete and truncated versions of the polar wander equations, *J. geophys. Res.*, **89,** 7609–7620.

Stein, S. & Gordon, R. G., 1984. Statistical tests of additional plate boundaries from plate motion inversions, *Earth planet. Sci. Lett.*, **69,** 401–412.

Vogt, P. R. & Perry, R. K., 1981. *North Atlantic Ocean: Bathymetry and Plate Tectonic Evolution,* Geol. Soc. Am. Map and Chart Series, MC-35.